

## NET-INDUCING DIAMOND NANOPARTICLES WITH ADSORBED HYDROPHOBIC SARS-CoV-2 ANTIGENS SERVING AS VACCINE CANDIDATE

G. BILA, V. VOVK, V. UTKA, R. GRYTSKO,  
A. HAVRYLYUK, V. CHOPYAK, R. BILYY✉

Danylo Halytsky Lviv National Medical University, Lviv, Ukraine;  
✉e-mail: [r.bilyy@gmail.com](mailto:r.bilyy@gmail.com)

**Received:** 14 April 2024; **Revised:** 17 May 2024; **Accepted:** 25 July 2024

*This study addresses the current need for vaccine adjuvants able to induce an immune response to novel or mutated pathogens. It exploits the ability of nanodiamonds (ND) to induce the formation of neutrophil extracellular traps (NETs) triggering inflammation, accompanied by immune response to co-injected antigens. Hydrophobic nanodiamonds 10 nm in diameter were covered with 194 a.a. sequence of the receptor-binding domain of Spike protein of SARS-CoV-2 via passive adsorption. It was shown that antigen-covered ND induce activation of human neutrophils and stimulate NETs formation and ROS production. When used for immunization antigen-covered ND induce a long-lasting immune response in mice with prevailing IgG1 among antibody subclasses. The injected nanoparticles were sequestered by NETs and safely covered with connective tissues when examined 1 year after injection.*

**Key words:** nanodiamonds, neutrophil extracellular traps, ROS, SARS-CoV-2, S-protein, IgG1, adjuvants, vaccine.

The rapid and efficient development of a COVID vaccine has been the primary objective for numerous research teams during the initial months of the pandemic. However, after this first battle with unknown pathogens the research community realized how long is a pathway from pathogen identification towards efficient vaccine creation. Pan-coronavirus vaccines, vaccines against disease X (caused by unknown potential pathogen with high mortality) are becoming discussed as top world priority issues. While decoding the genetic information of a new virus can now be achieved relatively quickly, we still face challenges in promptly generating an immune response against synthetic fragments of the virus, the need to rapidly achieve immunity to a potential novel strain or pathogen. This issue arises because a robust immune response is typically triggered only when a potent adjuvant is present [1]. Conventionally, adjuvants in vaccines, such as alum compositions, form colloidal suspensions when co-injected with antigens, serving as depots for antigen release [2]. However, these adjuvants exhibit limited effectiveness, particularly when working with peptides, thus due to effectiveness and safety considerations, only a few are licensed to use

with humans [3]. In addition to eliciting a robust immune response, the adjuvant employed in a vaccine must also meet criteria of safety, cost-effectiveness, and scalability in production. In our previous study conducted in 2016, we presented compelling evidence that hydrophobic nanoparticles within the size range of 10 to 40 nm, including nanodiamonds (ND) and polystyrene nanoparticles, exhibit remarkable capabilities in inducing a potent immune response. These nanoparticles, upon contact with the plasma membrane, initiate cell death processes, particularly through the generation of neutrophil extracellular traps (NETs) in neutrophilic granulocytes. The cell death triggered by nanoparticles is self-limiting, as the NETs effectively encapsulate and sequester the stimulating agent [4], subsequently neutralizing pro-inflammatory cytokines [5]. Notably, this phenomenon was observed even in cases of sterile inflammation [6] and other naturally occurring nanocrystals [7]. Its mechanism is explained in detail in [8] and is due to membrane recovering upon contact with nanoparticles, not a specific receptor, thus allowing nanoparticles to trick our inborn protective mechanisms with the aim to generate a strong immune response. Independent calculations have further confirmed that

the size and surface properties of nanoparticles play a crucial role in causing membrane damage in cells [9]. The involvement of NETs has also been demonstrated in certain forms of traditional aluminum oxide when utilized as adjuvants [10, 11] and was recently proposed as an underlying mechanism for most particulate vaccines [12]. Covalent conjugation of the hydrophilic pan-coronaviral peptide within the HR2 region of S-protein to 10 nm-sized ND resulted in a strong immune response in mice [13]. However, most immunogenic peptides of SARS-CoV-2 have hydrophobic parts, and thus their solubility is a significant issue for the creation of an efficient vaccine. This is also true regarding most synthetic immunogenic peptides. To omit the need for additional steps of peptide conjugation potentially altering the chemistry of immunogenic epitope, here we proposed a relatively simple immobilization of coronaviral pro-teins/peptides by hydrophobic interaction with 10nm ND particles, resulting in injectable suspension covered with exposed hydrophilic amino acid residues. Such immunogenic composition was used to immunize laboratory mice and resulted in a strong and stable (240 day) immune response. The injected ND were sequestered by NETs and then covered with connective tissue in the body within 1 year of observation, suggesting their good biocompatibility.

These findings highlight the potential of utilizing hydrophobic ND as adjuvants due to their ability to induce an immune burst. By leveraging their unique properties, we may overcome the limitations associated with traditional adjuvants and facilitate the rapid and efficient generation of an immune response to synthetic peptide fragments of the COVID virus. This research provides a promising avenue for the development of safe, cost-effective, and scalable adjuvants for novel COVID vaccines or those to be made on-site using common laboratory equipment.

## Materials and Methods

**Materials.** Nanodiamonds were obtained from Merck (Diamond nanopowder, < 10 nm particle size, Nr. 636428, D10). Recombinant part of S-protein of SARS-CoV-2 with the sequence NITNLCPFGEVFNATRFASVYAWNKRKISNCVADYSVLYNSASF-STFKCYGVSPTKLNLDL-CFTNVYADSFVIRGDEVQRQIAPGQTGKIA-DYNYKLPDDFT-GCVIAWNSNNLDSKVGGNY-NYLYRLFRKSNLKPFRDISTEIQAGSTPC-NGVEGFNCYFPLQSYGFQPTNGVGYQPYRV-

VVLSFELLHAPATV with 99% purity was obtained from Explogen, Ukraine. The protein was expressed in *E. coli*, the culture was lysed and hydrophobic protein was dissolved in buffer containing 6 M guanidine chloride, 400 mM NaCl and 20 mM Tris-HCl (solubilizing buffer, SB). Hydrophilic part of peptide with the sequence of DDFTGCVIAWN-SNNLDSKVGGNYLYRLFRKSNLKPFRDISTEIQAG was obtained from ProteoGenix, France and was used for Delayed Type Hypersensitivity (DTH) study.

**Surface modification.** ND (10 mg) were mixed with SB buffer containing 1 mg of protein and sonicated in ultrasonic bath 40W, 22 kHz for 10 min at RT. ND-protein mixtures were centrifuged at 25 000 g and washed in PBS. Washing was repeated. Suspension was sonicated for 5 min immediately before injection.

**NETosis analysis.** Human granulocytes were isolated from heparinized venous blood of normal healthy donors by Lymphoflot (Bio-Rad) density gradient centrifugation, as described [5]. The granulocyte-rich layer on top of RBCs was taken and subjected to hypotonic lysis of RBCs. Isolated granulocytes were cultured in 96-well culture plates at  $5 \times 10^6$  cells per milliliter with special inducers of NETosis and with the fluorescent nucleic acid dye Sytox green (Life Technologies). The fluorescence was measured in kinetics for 3 h using BioAssay Reader HTS7000 Plus (Perkin Elmer), excitation 480/15 nm, emission 535/20 nm. ROS production in neutrophil population was analyzed with DHR123 assay as described [14]. Cells were analyzed using DXFlex Flow cytometer.

**Animals.** Studies involving animals, including housing and care, method of euthanasia, and experimental protocols were approved by the Ethical committee of Danylo Halytsky Lviv National Medical University, protocols 20191216/10, 20210622/6, all experiments were designed to comply with principles of the 3Rs (Replacement, Reduction and Refinement). Mice were housed in a temperature/humidity/light controlled environment, with both food and drinking water available ad libitum.

**Animal immunization.** Mice immunization was done as described previously [10]. A mixture of ND covered with pan-coronaviral protein was used for immunization. 1 mg of ND containing ~0.095 mg of adsorbed protein was injected per injection in 100  $\mu$ l of PBS. The DTH test [15] was performed 28 days after the 1<sup>st</sup> immunization by injection of

5 µg of peptide in PBS (50 µl) into the right hind paw. Injection of 50 µl of PBS into the left hind paw was used as a control. The thickness of the paw was measured with a caliper (B110T; Kroeplin Laengenmesstechnik) before the injection and 6, 24, 48, 72 and 96 h after it, as described previously [10]. Blood was collected from the mouse tail before the experiment started (day 0), before second immunization (day 14) and at the end of experiment (day 35). No more than 50 µl of blood was collected to prevent damage to the animal. Serum was isolated (usually 20 µl per mouse) and immediately frozen at -20°C.

**Microscopy and tissue analysis.** Animal tissues were fixed in 4% PFA solution. They were embedded, sliced into 5 µm thick sections, stained with H&E according to routine laboratory procedures and analyzed as described [16]. Fluorescent microscopy was performed with a BZ-X800 microscope (Keyence Corporation, Osaka, Japan). Z-stacks were performed to increase the depth of field. Post-processing of pictures and morphometry was performed employing Photoshop CS5 64Bit (Adobe, München, Germany). Transmission Electron Microscopy (TEM) images were recorded on a PEM-100-01 electron microscope (Ukraine) by the Laboratory of electron microscopy, LNMU.

**ELISA tests.** For testing anti-SARS-CoV-2 response immunosorbent NUNC maxisorp plates (Thermo Scientific, Waltham, USA) were coated with S-protein (50 µl of a 2 µg/ml solution) in an SB with pH adjusted to 10.0. All serum samples were diluted 1:1000 in the PBS-T and incubated at 37°C for 1 h, after that the plates were rewashed. For the determination of IgG antibody titres samples collected at day 35, after the second immunization, a series of dilutions were used. Goat anti-mouse IgG (H+L)-horseradish peroxidase (HRP) (109-035-003, Jackson ImmunoResearch) were diluted in washing buffer (1:15000), added to the plates, and incubated at room temperature for 1 h. After the corresponding washings, the assay was developed with 3,3',5,5'-tetramethylbenzidine (TMB) containing an excess of H<sub>2</sub>O<sub>2</sub> as a substrate (50 µl per well). The reaction was stopped with 50 µl/well of sulfuric acid (1 M). The absorbance was read at 450 nm/600 nm using a Perkin Elmer BioAssay reader HST7000 (Waltham, USA). For determination of antibody subclass compositions, specific antibodies against IgG1, IgG2a, IgG2b, IgG2c, IgG3, IgA, IgE, IgM (all from Southern Biotech, USA) were used. Anti-SARS-CoV-2 ELISA was additionally tested with reference

positive sera for COVID-19 diagnostics, and their signal was in the range of 0.45-0.60 OD. The CV between replicates was controlled to be <3%. Other ELISA parameters were controlled according to the best practice of ELISA analysis [17, 18] and our previous reports [19, 20].

**Data analysis.** The protein homology searches were done using Blast (NCBI) and PDB databases. To include the regions with resolved structures in our searches, we used SEQATOMS (<http://www.bioinformatics.nl/tools/seqatoms/>) [21]. Protein structures were visualized and aligned using PyMOL (<https://pymol.org/>). ELISA testing was performed in duplicate using 2 technical replicates for each analysis (coefficient of variation [CV] always <3%). The data were normalized between plates using positive controls and corrected for the background signal of secondary antibodies on each plate, then the mean values were calculated. The mean values were used to construct data on the figures. For comparisons between two groups, the Mann-Whitney U-test for numerical variables was used. All analyses were performed using Excel 2016 (Microsoft Corp., Redmond, WA, USA) and Prism 8.2 (GraphPad, San Diego, USA) software. A *P*-value of ≤0.05 was considered statistically significant. Three levels of significance are depicted in the figures by asterisks: \**P* < 0.05; \*\**P* < 0.01; \*\*\**P* < 0.001.

## Results

### Covering nanodiamonds with SARS-CoV-2 antigen

**Antigen selection.** To induce immunity towards SARS-CoV-2 antigen we utilized 194 a.a. sequence of receptor-binding domain (RBD) of Spike (S) protein of SARS-CoV-2. This part of SARS-CoV-2 is considered to be immunogenic and is distinct from other coronaviruses, ensuring the generation of specific anti-SARS-CoV-2 immunity [22]. The protein part selected for immunization is shown in Fig. 1, A. It was expressed in the *E. coli* BL21 (DE3) system by Exploregen LLC, UA. The protein was stained in the insoluble bacterial lysate fraction, from where it was purified by gradually washing out the soluble proteins until the antigen was dissolved in SB, reaching >99% purity when checked by SDS-PAGE. The antigen was effectively used to discriminate convalescent COVID patients against normal healthy donors in ELISA assay [23].

**Adsorption of antigen of nanodiamonds.** Mixing D10 nanoparticles with antigen, sonication

and purification of suspensions allowed us to obtain a relatively stable suspension of D10-antigen. Up to 0.8 mg of protein could be immobilized on 1 mg of D10 nanoparticles. Electron microscopy of nanodiamond particles before (Fig. 1, B) and after (Fig. 1, C) protein adsorption revealed the formation of a protein coat on the surface of the particles. Most important, obtained conjugate could be sonicated to provide a suspension, stable for at least 1 hour in saline-based solutions, needed for cellular assays and immunizations experiment.

### Antigen-covered nanodiamonds induce activation of human neutrophils

*NETs formation upon the interaction with nanoparticles.* The created antigen-covered ND were incubated with a population of polymorphonuclear neutrophils isolated from peripheral venous blood of normal healthy donors and used for NET-inducing test using Sytox Green as a marker for DNA externalization. Obtained data demonstrated that the nanodiamond component was a primary cause responsible for DNA externalization. As both nanodiamond covered and uncovered with protein enveloped induced NETs formation (Fig. 2, A). Upon isolation from the blood untreated PMN cells are subject to spontaneous DNA externalization at a slow rate, which served as a control. Both ND and ND-antigen particles induced statistically significant DNA externalization already after 180 min of co-incubation.

*ROS production upon contact with nanoparticles.* The amount of ROS produced by neutrophils upon the contact with ND was measured with DHR123 assay. The mean level of ROS in the un-

treated PMN population, determined in 3 different donors, was shown to be  $168.08 \pm 24.32$  MFI, that of PMN treated with ND alone was  $454.42 \pm 42.21$ , and upon the action of ND covered with antigen it raised to  $618.24 \pm 54.21$ . Representative plots are shown in Fig. 2, B. Thus, addition of antigen coat to nanoparticle stimulated ROS production of PMN cells and served as additional trigger needed for efficient immune response.

### Antigen-covered nanodiamonds induce strong and long lasting immune response in mice

*Dynamics of humoral immune response evaluated by IgG titers.* The ability to quickly generate sufficient IgG titers is crucial for every vaccine candidate. Thus we evaluated levels of specific anti-S-protein antibodies of different IgG classes in the blood serum of mice immunized with S-protein-coated ND particles. ND particles were injected subcutaneously and were previously shown to induce local self-limiting inflammation with abundant NETs-formation in the place of injection [6, 24]. Immunization was done on day 1 and day 15 according to the scheme described in [10], and serum was collected and analyzed on day 14 and day 35. No significant levels of specific anti-S-protein antibodies were formed at day 14; however, after the second (boost) immunization, their levels were significantly increased at day 35 post 1<sup>st</sup> immunization, thus indicating a fast and strong humoral immune response towards the antigen.

*Cellular immune response to ND-antigen particles.* To test humoral immune response we used mice population immunized twice on day 1 and day

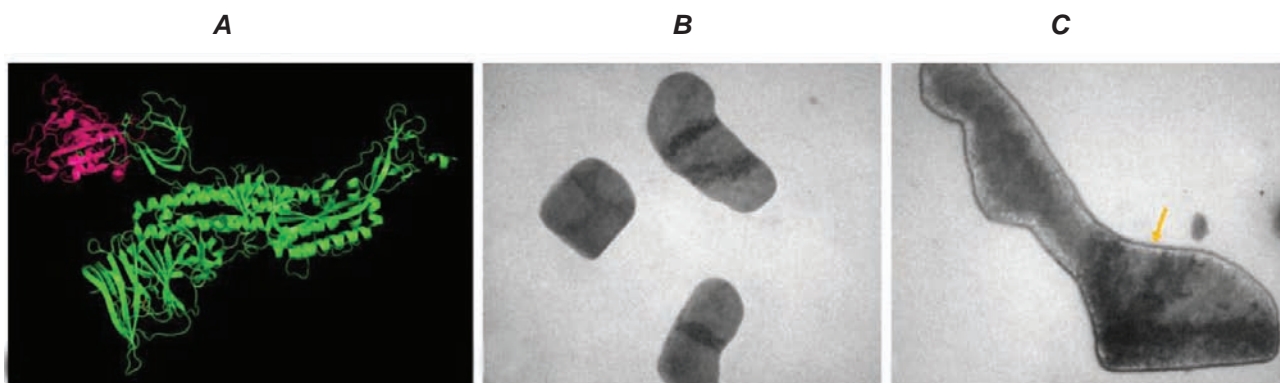


Fig. 1. Adsorption of proteins on diamond nanoparticles. A – part of S-protein of SARS-CoV-2 shown in red was expressed for further analysis. It consisted of 194 a.a. Diamond nanoparticles before (B) and after (C) adsorption of protein mixture,  $\times 5000$ . The latter made a noticeable coat (yellow arrow) on the surface of ND

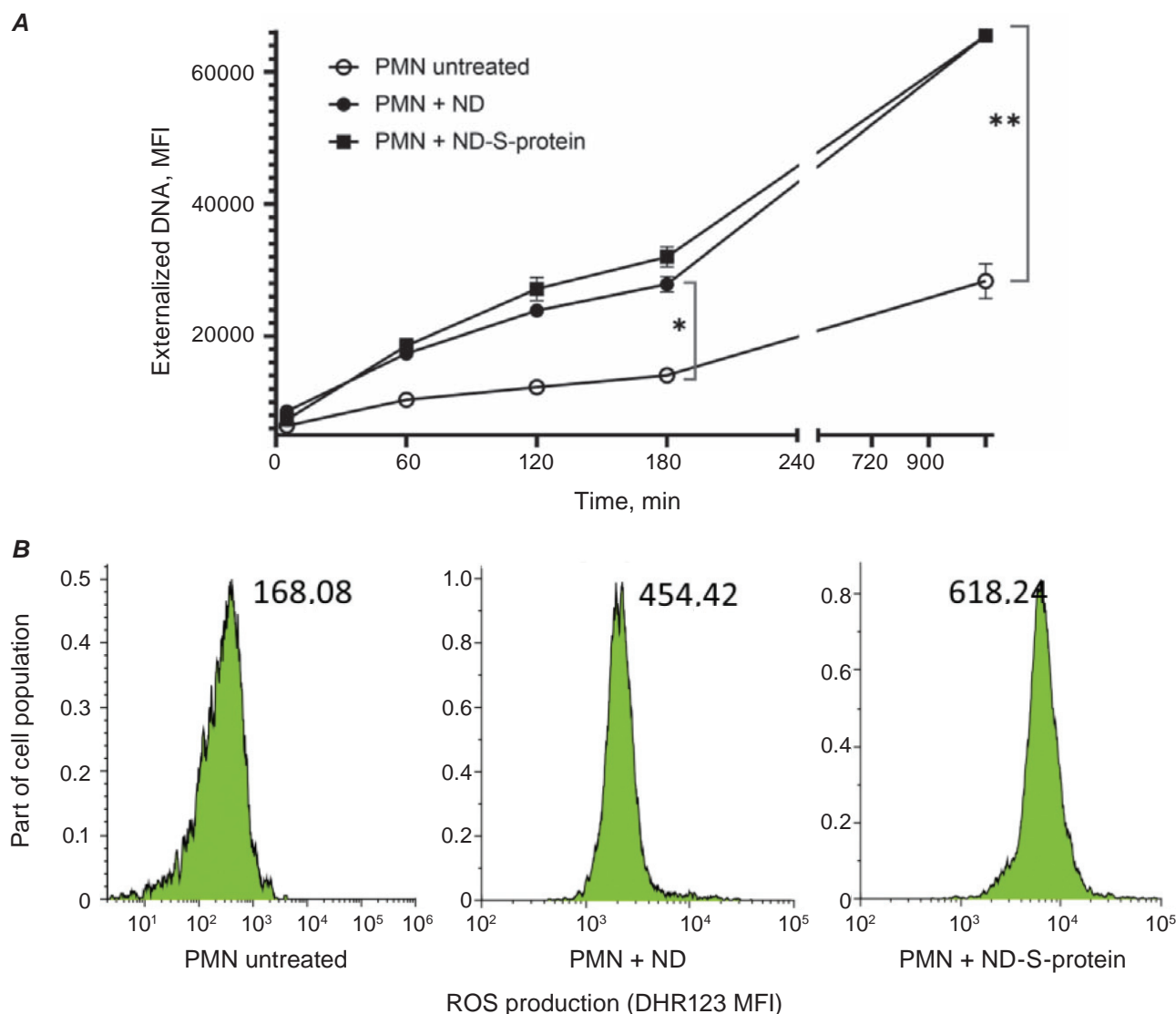


Fig. 2. Effect of ND-antigen composition on DNA externalization (A) and ROS production (B) by human PMN cells isolated from healthy donors

15 and on day 28 we injected 5  $\mu$ g of soluble part of S-protein in saline (total volume of 50  $\mu$ l) into the footpad of the animal. Saline alone was injected into opposite footpad and served as a normalization control. Antigen presentation in the footpad induced T-cell-mediated delayed type hypersensitivity reaction revealed in footpad swelling. Specific footpad swelling (data for antigen minus those for saline alone) indicated strong and rapid DHT cellular response 6 h after injection, reaching more than 35% of initial size, with a gradual decrease in magnitude upon 24 and 48 h, at 96 h (Fig. 3, B).

*IgG1 prevail among antibody subclasses induced by antigen-covered ND.* To determine a subclass of IgG antibodies induced upon antigen absorp-

tion on ND and to compare to antigen used without adjuvant we used a set of class-specific antibodies in ELISA assay. Obtained data indicated that sorption on nanodiamond adjunct has a major effect on enhancing the production of IgG1 subclass antibodies, as well as an increase in IgG2b and IgG3 antibody subclasses (data significant in all cases). No effect was shown on IgG2a, IgA and IgE antibody classes (Fig. 3, C).

*Obtained IgG levels were stable for at least 240 in mice blood.* To answer the question on how long antibodies are maintained in blood of mice after a course of 2 immunization, we performed long-term monitoring of antibody titers in immunized mice population. For this reason, ten 12-week-old mice

were immunized and continuously checked for antibody levels in their blood during 240 days (Fig. 3, D). Obtained data suggest that antibody production reached its peak in the mice organism within 90 days after the first immunization. The constant increase in antibody levels observed for 90 days demonstrated strong antigen-depo effect realized by ND-protein adjuvants. Obtained antibody levels were maintained for up to 240 days during the experiment.

### Long-term tissue biocompatibility of ND used as adjuvants

To assess the long-term safety of injected nanodiamonds (ND) as adjuvants, we conducted a year-long observation on mice receiving two doses of nanodiamonds. Throughout the study, we regularly monitored their weight, observed behavior, and assessed typical biochemical parameters in urine, including glucose, protein, microalbumin, and ketones

employing rapid urine tests. In all cases, we found no deviations from the data observed in normal mice or mice treated solely with peptide antigen.

After one year, we euthanized the mice and meticulously examined the injection sites to observe the presence and distribution of ND particles. These particles, easily identifiable due to their black color, were localized within specific granuloma-like structures, reaching up to 2 mm in diameter within the skin (Fig. 4, A and B). Corresponding skin sections were removed, photographed, fixed, and subjected to conventional histological analysis (Fig. 4, C).

The ND were found enclosed in capsules, covered with connective tissue. To confirm the presence of diamond nanoparticles, their intrinsic fluorescence was checked and confirmed in the far-red range of the spectra (Fig. 4, D). Inside the capsules, agglomerates of particles were observed within phagocytic cells. Surrounding these aggregates was a layer of

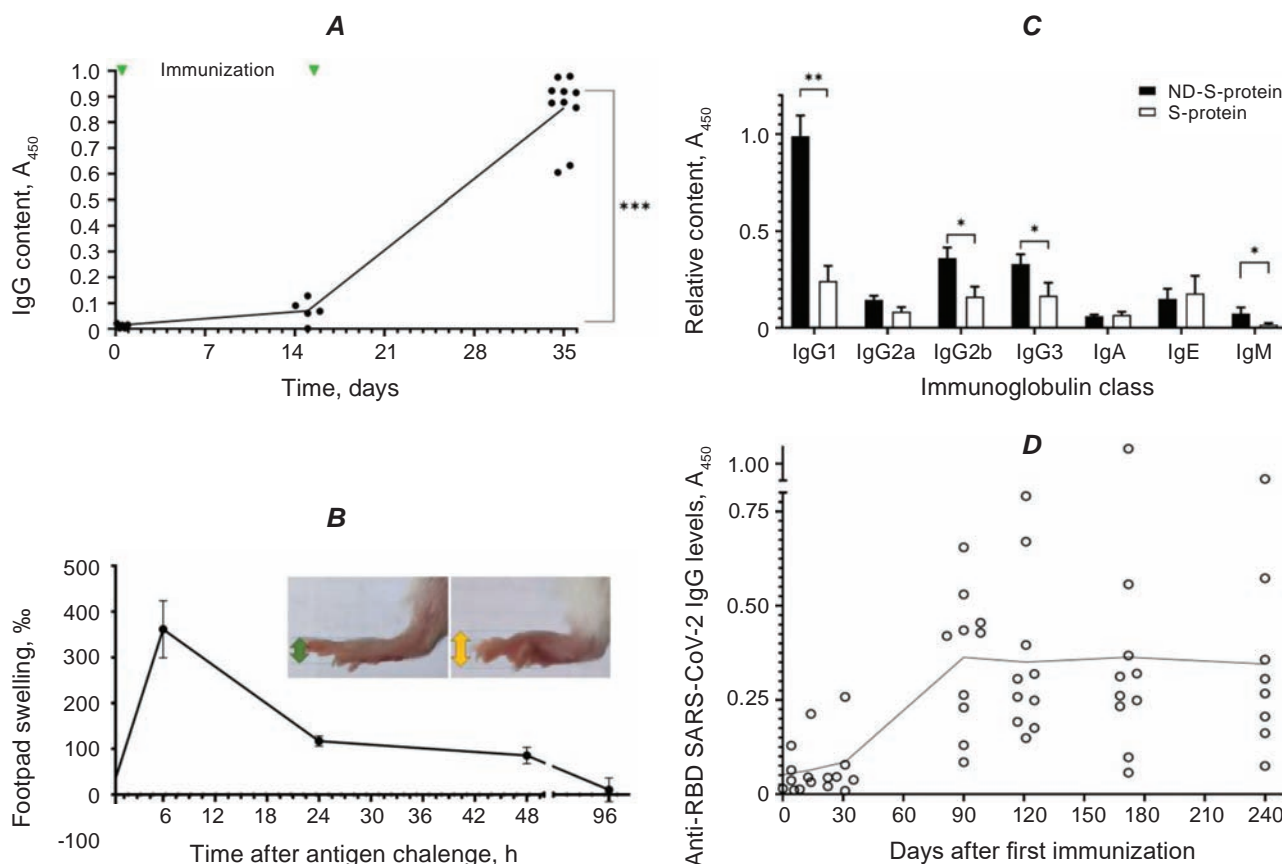


Fig. 3. Immune response of antigen-covered ND. **A** – humoral immune response during the course of 2 immunizations. **B** – cellular immune response detected as DTH reaction via monitoring footpad swelling. **C** – class and subclass composition of antibodies produced upon immunization with S-protein adsorbed on ND and in solution. Insert demonstrate the height of the footpad before (green) and after swelling (yellow). **D** – levels of obtained antibodies during 240 days post-immunization

connective tissue composed of fibroblasts and some infiltrating leukocytes (Fig. 4, *E* and *F*). Additionally, single phagocytic cells in this area (Fig. 4, *G*) contained some small fluorescent particulate particles in their cytoplasm.

No signs of pus, edema, bleeding, or other adverse effects were observed in the tissue. The layer of connective tissue around nanodiamonds appeared well-formed, containing all cellular and fiber components of dense connective tissue (irregular type). These findings indicate good biocompatibility and the absence of adverse effects following the injection of diamond nanoparticles.

## Discussion

The recent COVID pandemic has underscored humans' vulnerability to novel and emerging viruses. While mRNA vaccines are affordable and potent, their careful design demands significant time and access to state-of-the-art research and production facilities. Recent findings suggest that the mechanism of action of many particulate adjuvants, including alum, is connected with the activation of neutrophils and/or NETs, reviewed in [12]. Leveraging the recently discovered phenomenon of a robust immune burst due to neutrophil activation with nanoparticles, we present a rapid and efficient

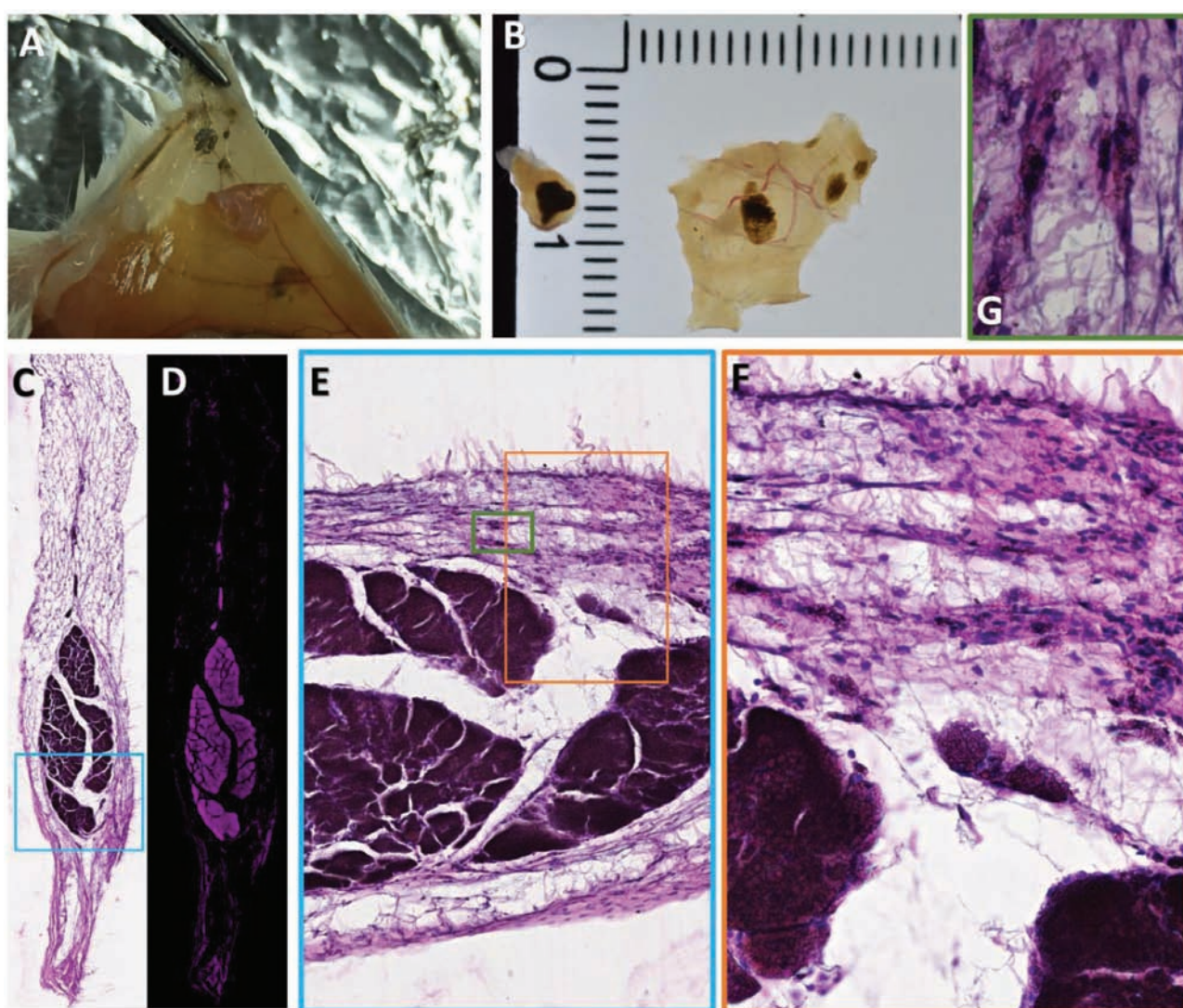


*Fig. 4. Localization of diamond nanoparticles in mice tissue 1-year post-injection. A, B – macrophotographs of the skin at the place of injection. C – histology of isolated skin area, staining with H&E. D – the sample at C analyzed for fluorescence using ex. at 640/20 and em. at 700/40 nm. E, F, G – sequential magnification of the connective tissue, formed around the particulate aggregates demonstrated formed cells and fibers, and some phagocytes (G) containing aggregated particles. The color frame corresponds to the magnified area shown*

method of adding protein antigens to hydrophobic nanoparticles. The ability to produce oxidative bursts upon contact with nanoparticles is critical for triggering the immune response [6], formation of aggregated NETs and subsequent resolution of inflammation [5]. However, recent findings suggest that under low-grade inflammation, interaction of nanodiamonds with neutrophils results in lowered ROS production [25], probably due to exhaustion of oxidative machinery under chronic inflammatory conditions. This limitation in patients with low-grade inflammation can be overcome by increasing antigen dose as ND possess a high surface area allowing immobilization of a very high amount of antigens. Being composed solely of carbon atoms, nanodiamonds lack specific receptors in the cells of the body, minimizing the risk of triggering immune cell activation or hyper-reaction.

In our study, we utilized a 194-amino acid SARS-CoV-2 peptide, a component of the S-protein, to induce an immune response. Despite the inherent immunogenicity of this S-protein segment [26, 27], its production in artificial expression systems often leads to improper folding and poor solubility. Recognizing the hydrophobic and hydrophilic nature of proteins, adsorption on the surface of superhydrophobic diamonds exposes the hydrophilic parts of the synthetic peptide, stabilizing the nanoparticle suspension for injection into tissues.

This approach yielded high antibody levels and a robust cellular immune response. The acute delayed-type hypersensitivity (DTH) reaction and sustained stability of anti-body titers in the body suggest the generation of immune cells responsive to the presented antigen epitopes. Notably, achieving substantial antibody levels after the second immunization using diamond-based adjuvants makes them a viable option for situations where repeated revaccination is challenging, as demonstrated in recent reports requiring three immunizations with other adjuvant platforms such as outer membrane vesicles [28].

The persistence of antibody titers over 240 days, considering the typical lifespan of mice, highlights the stability of the immune response. The known property of nanodiamonds to fluoresce [29] facilitated tracking within the body, demonstrating high compatibility with body tissues even one year

after injection. Fluorescence of nanodiamonds can also be used for monitoring their fate on the site of injection during vaccination using *in vivo* NIR-fluorescence imaging [30] or for specific targeting of pathologic cells [31].

The significant advantage of this approach lies in its simplicity and the minimal equipment required for on-demand vaccine creation against novel protein threats, whether bacterial or viral. Following the isolation and sequencing of pathogen DNA, the corresponding polypeptide can be synthesized and mixed with prepared nanodiamonds. These stable substances are easily transportable, making the approach suitable for remote missions and rapid responses to emerging pathogens or their strains.

*Conclusions.* In conclusion, the adsorption of poorly soluble peptides and proteins on nanodiamonds leads to the creation of highly immunogenic vaccine compositions. These compositions effectively induce a robust and long-lasting immune response towards adsorbed proteins through the activation of neutrophil extracellular traps (NETs) formation by nanodiamonds. This innovative approach holds promise for the development of potent vaccines with enduring immunogenicity able to effectively fight emerging pathogens.

*Patents.* The data reported in this paper are protected by UA (PCT) patent application No. a2023 05659 “Method of inducing an immune response toward hydrophobic peptides”.

*Data availability statement.* Data are available on request due to patenting restrictions.

*Conflict of interest.* The authors have completed the Unified Conflicts of Interest form at [http://ukrbiochemjournal.org/wp-content/uploads/2018/12/coi\\_disclosure.pdf](http://ukrbiochemjournal.org/wp-content/uploads/2018/12/coi_disclosure.pdf) and declare no conflict of interest.

*Funding.* This research was funded by Ministry of Health of Ukraine, grant 0122U000974, Imaging was done using infrastructure established under National Research Foundation of Ukraine grant 2020.02/0131.

*Acknowledgments.* We want to thank Andriy Rabets for his technical assistance and Dr. Markiyan Samborskyy for his guidance with bioinformatics analysis.

## НАНОДІАМАНТИ ЗДАТНІ ДО ІНДУКЦІЇ НЕЙТРОФІЛЬНИХ ПОЗАКЛІТИННИХ ПАСТОК ІЗ АДСОРБОВАНИМИ ГІДРОФОБНИМИ АНТИГЕНАМИ SARS-CoV-2 НА ПОВЕРХНІ ЯК ПОТЕНЦІЙНІ КАНДИДАТИ ВАКЦИН

Г. Біла, В. Вовк, В. Утка, Р. Грицко,  
А. Гаврилюк, В. Чоп'як, Р. Білий✉

Львівський національний медичний університет  
імені Данила Галицького, Львів, Україна;  
✉e-mail: r.bilyy@gmail.com

Дане дослідження спрямоване на пошук затребуваних ад'ювантів вакцин, здатних викликати імунну відповідь на нових або мутованих патогенів. Воно описує здатність нанодіамантів (ND) індукувати утворення позаклітинних нейтрофільних пасток (НПП), що спричиняє запалення, яке супроводжується імунною відповіддю на одночасно введені антигени. Гідрофобні нанодіаманти розміром 10 нм, шляхом пасивної адсорбції були покриті поліпептидом послідовністю з 194 амінокислот, що відповідає домену зв'язування з рецептором Spike-протеїну SARS-CoV-2. Було показано, що вкриті антигеном ND індукують активацію людських нейтрофілів та стимулюють утворення НПП і продукцію АФК. При використанні для імунізації вкриті антигеном ND викликають тривалу імунну відповідь у мишей з переважанням IgG1 серед підкласів антитіл. Ін'єктовані наночастинки були секвестровані НПП і безпечно покриті сполучною тканиною при дослідженні через 1 рік після ін'єкції.

**Ключові слова:** нанодіаманти, нейтрофільні позаклітинні пастки, АФК, SARS-CoV-2, IgG1, ад'юванти, вакцина.

### References

- Pollard AJ, Bijker EM. A guide to vaccinology: from basic principles to new developments. *Nat Rev Immunol*. 2021; 21(2): 83-100.
- Lindblad EB. Aluminium compounds for use in vaccines. *Immunol Cell Biol*. 2004; 82(5): 497-505.
- Apostólico JdeS, Lunardelli VAS, Coirada FC, Boscardin SB, Rosa DS. Adjuvants: Classification, Modus Operandi, and Licensing. *J Immunol Res*. 2016; 2016: 1459394.
- Bilyy R, Bila G, Vishchur O, Vovk V, Herrmann M. Neutrophils as Main Players of Immune Response Towards Nondegradable Nanoparticles. *Nanomaterials (Basel)*. 2020; 10(7): 1273.
- Schauer C, Janko C, Munoz LE, Zhao Y, Kienhöfer D, Frey B, Lell M, Manger B, Rech J, Naschberger E, Holmdahl R, Krenn V, Harrer T, Jeremic I, Bilyy R, Schett G, Hoffmann M, Herrmann M. Aggregated neutrophil extracellular traps limit inflammation by degrading cytokines and chemokines. *Nat Med*. 2014; 20(5): 511-517.
- Biermann MHC, Podolska MJ, Knopf J, Reinwald C, Weidnerv, Maueröder C, Hahn J, Kienhöfer D, Barras A, Boukherroub R, Szunerits S, Bilyy R, Hoffmann M, Zhao Y, Schett G, Herrmann M, Munoz LE. Oxidative Burst-Dependent NETosis Is Implicated in the Resolution of Necrosis-Associated Sterile Inflammation. *Front Immunol*. 2016; 7: 557.
- Desai J, Foresto-Neto O, Honarpisheh M, Steiger S, Nakazawa D, Popper B, Buhl EM, Boor P, Mulay SR, Anders HJ. Particles of different sizes and shapes induce neutrophil necroptosis followed by the release of neutrophil extracellular trap-like chromatin. *Sci Rep*. 2017; 7(1): 15003.
- Bila G, Rabets A, Bilyy R. Nano- and Micro-particles and Their Role in Inflammation and Immune Response: Focus on Neutrophil Extracellular Traps. In *Biomedical Nanomaterials*; Springer International Publishing: Cham, 2022. P. 149-170.
- Agudo-Canalejo J, Lipowsky R. Critical particle sizes for the engulfment of nanoparticles by membranes and vesicles with bilayer asymmetry. *ACS Nano*. 2015; 9(4): 3704-3720.
- Bilyy R, Paryzhak S, Turcheniuk K, Dumych T, Barras A, Boukherroub R, Wang F, Yushin G, Szunerits S. Aluminum oxide nanowires as safe and effective adjuvants for next-generation vaccines. *Mater Today*. 2019; 22: 58-66.

11. Stephen J, Scales HE, Benson RA, Erben D, Garside P, Brewer JM. Neutrophil swarming and extracellular trap formation play a significant role in Alum adjuvant activity. *NPJ Vaccines*. 2017; 2: 1.
12. Vaseruk A, Bila G, Bilyy R. Nanoparticles for stimulation of neutrophil extracellular trap-mediated immunity. *Eur J Immunol*. 2024; 54(4): e2350582.
13. Bilyy R, Pagneux Q, François N, Bila G, Grytsko R, Lebedin Y, Barras A, Dubuisson J, Belouzard S, Séron K, Boukherroub R, Szunerits S. Rapid Generation of Coronaviral Immunity Using Recombinant Peptide Modified Nanodiamonds. *Pathogens*. 2021; 10(7): 861.
14. Bekeschus S, Winterbourn CC, Kolata J, Masur K, Hasse S, Bröker BM, Parker HA. Neutrophil extracellular trap formation is elicited in response to cold physical plasma. *J Leukoc Biol*. 2016; 100(4): 791-799.
15. Allen IC. Delayed-type hypersensitivity models in mice. *Methods Mol Biol*. 2013; 1031: 101-107.
16. Bila G, Schneider M, Peshkova S, Krajnik B, Besh L, Lutsyk A, Matsyura O, Bilyy R. Novel approach for discrimination of eosinophilic granulocytes and evaluation of their surface receptors in a multicolor fluorescent histological assessment. *Ukr Biochem J*. 2020; 92(2): 99-106.
17. Kiessig S, Abel U, Risse P, Friedrich J, Heinz F, Kunz C. Problems of cut-off level determination in enzyme immunoassays: the case of TBE-ELISA. *Klin Lab*. 1993; 39(11): 877-886.
18. Crowther JR. The ELISA Guidebook: Second Edition (Methods in Molecular Biology). Humana Press: Totowa, NJ, 2009; Vol. 516.
19. Biermann MHC, Boeltz S, Pieterse E, Knopf J, Rech J, Bilyy R, van der Vlag J, Tincani A, Distler JHW, Krönke G, Schett GA, Herrmann M, Muñoz LE. Autoantibodies Recognizing Secondary Necrotic Cells Promote Neutrophilic Phagocytosis and Identify Patients With Systemic Lupus Erythematosus. *Front Immunol*. 2018; 9: 989.
20. Bozhenko M, Boichuk M, Bila G, Nehrych T, Bilyy R. Freezing influences, the exposure of IgG glycans in sera from multiple sclerosis patients. *Ukr Biochem J*. 2020; 92(2): 21-31.
21. Brandt BW, Heringa J, Leunissen JAM. SEQATOMS: a web tool for identifying missing regions in PDB in sequence context. *Nucleic Acids Res*. 2008; 36(Web Server issue): W255-W259.
22. Ju B, Zhang Q, Ge J, Wang R, Sun J, Ge X, Yu J, Shan S, Zhou B, Song S, Tang X, Yu J, Lan J, Yuan J, Wang H, Zhao J, Zhang S, Wang Y, Shi X, Liu L, Zhao J, Wang X, Zhang Z, Zhang L. Human neutralizing antibodies elicited by SARS-CoV-2 infection. *Nature*. 2020; 584(7819): 115-119.
23. Rabets A, Bila G, Grytsko R, Samborskyy M, Rebets Y, Vari SG, Pagneux Q, Barras A, Boukherroub R, Szunerits S, Bilyy R. The Potential of Developing Pan-Coronaviral Antibodies to Spike Peptides in Convalescent COVID-19 Patients. *Arch Immunol Ther Exp (Warsz)*. 2021; 69(1): 5.
24. Muñoz LE, Bilyy R, Biermann MHC, Kienhöfer D, Maueröder C, Hahn J, Brauner JM, Weidner D, Chen J, Scharin-Mehlmann M, Janko C, Friedrich RP, Mielenz D, Dumych T, Lootsik MD, Schauer C, Schett G, Hoffmann M, Zhao Y, Herrmann M. Nanoparticles size-dependently initiate self-limiting NETosis-driven inflammation. *Proc Natl Acad Sci USA*. 2016; 113(40): E5856-E5865.
25. Bila G, Vishchur O, Vovk V, Vari S, Bilyy R. Neutrophil activation at high-fat high-cholesterol and high-fructose diets induces low-grade inflammation in mice. *Ukr Biochem J*. 2024; 96(2): 27-37.
26. Ahmed SF, Quadeer AA, McKay MR. Preliminary Identification of Potential Vaccine Targets for the COVID-19 Coronavirus (SARS-CoV-2) Based on SARS-CoV Immunological Studies. *Viruses*. 2020; 12(3): 254.
27. Low JS, Vaqueirinho D, Mele F, Foglierini M, Jerak J, Perotti M, Jarrossay D, Jovic S, Perez L, Cacciatore R, Terrot T, Pellanda AF, Biggiogero M, Garzoni C, Ferrari P, Ceschi A, Lanzavecchia A, Sallusto F, Cassotta A. Clonal analysis of immunodominance and cross-reactivity of the CD4 T cell response to SARS-CoV-2. *Science*. 2021; 372(6548): 1336-1341.
28. Croia L, Boscato Sopotto G, Zanella I, Caproni E, Gagliardi A, Tamburini S, König E, Benedet M, Di Lascio G, Corbellari R, Grandi A, Tomasi M, Grandi G. Immunogenicity of *Escherichia coli* Outer Membrane Vesicles: Elucidation of Humoral Responses against OMV-Associated Antigens. *Membranes (Basel)*. 2023; 13(11): 882.
29. Demchenko AP, Dekaliuk MO. Novel fluorescent carbonic nanomaterials for sensing and imaging. *Methods Appl Fluoresc*. 2013; 1(4): 042001.

30. Demchenko AP. Fluorescence Detection Techniques. *Introd Fluoresc Sens.* 2015: 69-132.
31. Ghanimi Fard M, Khabir Z, Reineck P, Cordina NM, Abe H, Ohshima T, Dalal S, Gibson BC, Packer NH, Parker LM. Targeting cell surface glycans with lectin-coated fluorescent nanodiamonds. *Nanoscale Adv.* 2022; 4(6): 1551-1564.